

Structure Validation of Natural Products by Quantum-Mechanical GIAO Calculations of ^{13}C NMR Chemical Shifts**

Giampaolo Barone,^[b] Luigi Gomez-Paloma,^[a] Dario Duca,^[b] Arturo Silvestri,^[b] Raffaele Riccio,^[a] and Giuseppe Bifulco*^[a]

In memory of our colleague and long-time friend Professor Guido Sodano

Abstract: Geometry optimization and GIAO (gauge including atomic orbitals) ^{13}C NMR chemical shift calculations at Hartree–Fock level, using the 6-31G(d) basis set, are proposed as a tool to be applied in the structural characterization of new organic compounds, thus providing useful support in the interpretation of experimental NMR data. Parameters related to linear correlation plots of computed versus experimental ^{13}C NMR chemical shifts for fourteen

low-polar natural products, containing 10–20 carbon atoms, were employed to assess the reliability of the proposed structures. A comparison with the hybrid B3LYP method was carried out to evaluate electron correlation contributions to the calculation of ^{13}C NMR

chemical shifts and, eventually, to extend the applicability of such computational methods to the interpretation of NMR spectra in apolar solutions. The method was tested by studying three examples of revised structure assignments, analyzing how the theoretical ^{13}C chemical shifts of both correct and incorrect structures matched the experimental data.

Keywords: ab initio calculations • NMR spectroscopy • natural products • GIAO • structure elucidation

Introduction

A number of papers have recently appeared in the literature concerning the calculation of NMR chemical shift (CS) by quantum-chemistry methods.^[1–6] These papers indicate that geometry optimization is a crucial factor in an accurate determination of computed NMR chemical shift. Moreover, it is known that the B3LYP DFT method adequately takes into account electron correlation contributions, which are especially important in systems containing extensive electron conjugation and/or electron lone pairs.^[5] However, considering that as molecular size increases, computing-time limitations are introduced for obtaining optimized geometries at the DFT level, it was proposed that the single-point calculation of

magnetic shielding by DFT methods was combined with a fast and reliable geometry-optimization procedure at the molecular mechanics level.^[5]

Herein we undertake the calculation of ^{13}C chemical shift, relative to tetramethylsilane, of organic compounds with molecular weight in the range 150–250 Dalton, by the ab initio Hartree–Fock (HF) method, after full-geometry optimization at the same level of theory. The choice of ab initio methods for geometry optimization was suggested by the up-to-date availability of computational methods and low cost hardware resources, which undoubtedly overcome the need to use empirical force fields or semiempirical methods for finding reliable geometries for broad classes of molecules. Our aim is to provide valid computational support to the structural characterization of natural products containing up to 20 carbon atoms, whose NMR spectra are usually recorded in the solution phase. ^{13}C NMR chemical shifts are particularly suitable for this method of analysis because they are spread over a larger spectral window than, for example, ^1H NMR chemical shifts.

The bottleneck in the application of quantum-chemistry methods for structure determination of solute molecules, is essentially the combination of 1) inherent computational limitations, strictly related to the size of the studied system and the accuracy of the theoretical approach, and 2) bulk effects, mainly related to the interaction of the probe molecule with the solvent. With regard to the first point, the

[a] Dr. G. Bifulco, Prof. L. Gomez-Paloma, Prof. R. Riccio
Dipartimento di Scienze Farmaceutiche
Università di Salerno
Via Ponte don Melillo, 84084 Fisciano, Salerno (Italy)
Fax (+39) 089-962828
E-mail: bifulco@unisa.it

[b] Dr. G. Barone, Prof. D. Duca, Prof. A. Silvestri
Dipartimento di Chimica Inorganica ed Analitica “S. Cannizzaro”
Università di Palermo
Viale delle Scienze, Parco d’Orleans II, 90128 Palermo (Italy)

[**] GIAO = gauge including atomic orbitals.

Supporting information for this article is available on the WWW under <http://www.chemeurj.org> or from the author.

current development of computer facilities and computational methods permits, especially for atoms of the first two rows of the periodic table, the use of increasingly extended basis sets at either HF, DFT, or post-HF methods for ^{13}C NMR calculations.^[6] Concerning the second point, the treatment of solvent effects and, more generally, of intermolecular interactions is not currently straightforward and pertains subjectively to the particular system under study.^[1, 6]

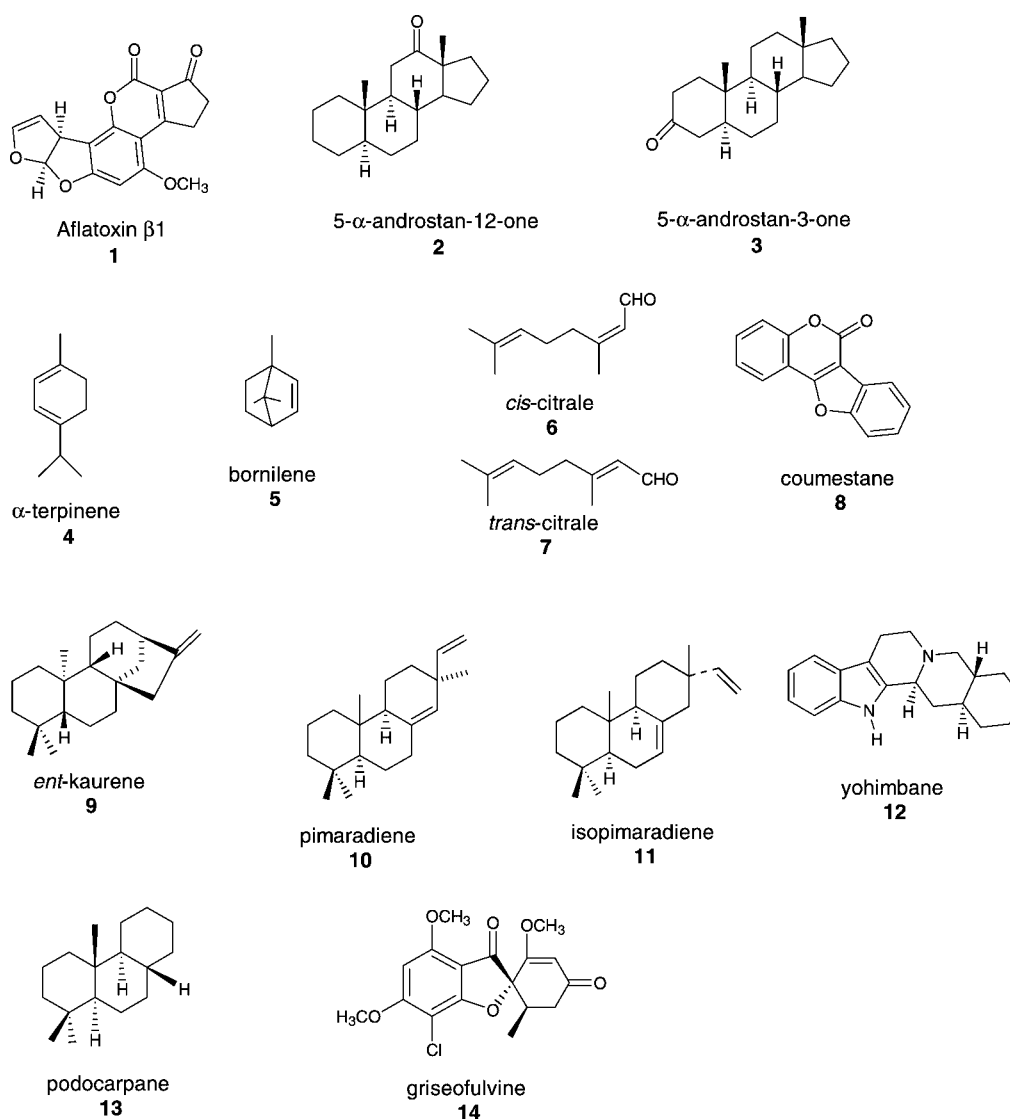
The development of new NMR equipment and techniques that has occurred over the last few years has propelled NMR spectroscopy to become the leading technique for the structure elucidation of organic compounds in solution. Nevertheless, in the field of natural products, even with the aid of the most powerful multi-dimensional analyses, sometimes the small amount of sample available and more often the intrinsic structural complexity can lead to erroneous or ambiguous conclusions.^[7]

Herein we focus on a number of low-polar organic compounds (Scheme 1), whose ^{13}C NMR spectra were typically recorded in deuterated chloroform solution. Indeed, for this class of compounds, we neglected the solvent effects in

our calculations, with the heuristic assumption that the solution structure is not, or is only very slightly, perturbed by the presence of the low-polarity solvent. The findings confirmed such a hypothesis.

Here we show the capability and limits of the HF method and the improvements made at the higher B3LYP level. A comparison between calculated and experimental chemical shifts of compounds with known structures^[8] shows that the computed chemical shifts are in good-to-excellent agreement with the experimental data. The NMR spectrum interpretation method is tested on three cases in which misinterpretation of experimental data led to erroneous structure determinations.^[7, 9, 10]

Interestingly, it was observed that electron correlation contributions were more important for species showing ^{13}C NMR signals in the low-field region of the spectrum. This observation can be used as a rule of thumb for using post-HF methods for the calculation of ^{13}C NMR chemical shifts. In the following paper in this issue,^[11] we extend the method to study the challenging field of flexible apolar compounds possessing stereogenic centers.

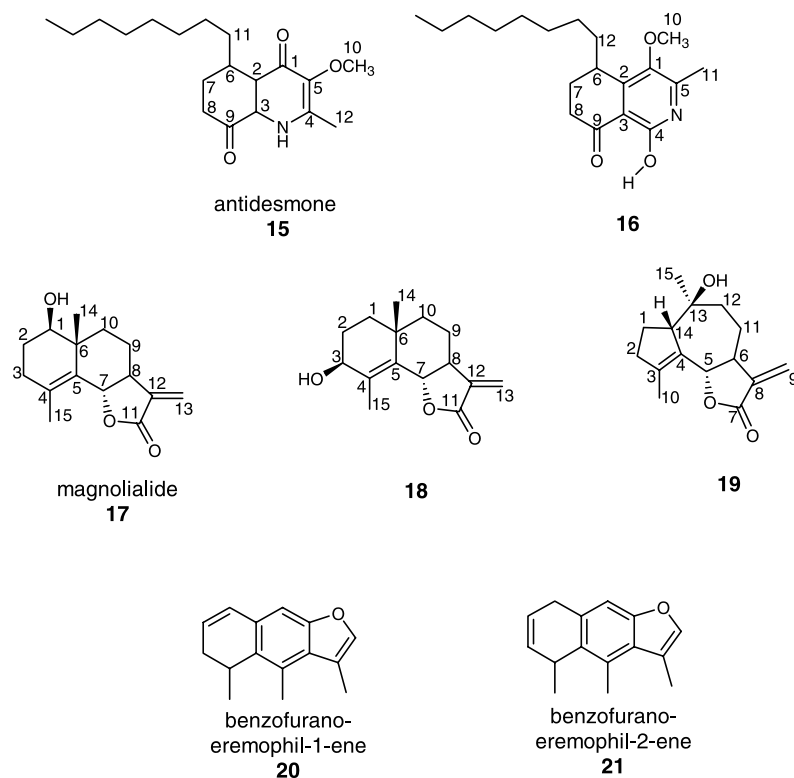


Scheme 1. Chemical structures of compounds **1–14**.^[8]

Results and Discussion

The ^{13}C chemical shift values, calculated for the optimized structures of the compounds shown in Scheme 1 and Scheme 2 were plotted against the corresponding experimental ^{13}C chemical shift values reported in the literature.^[7–10] These compounds, characterized by the absence of conformational isomerism, were selected among low-polar natural products with rigid frameworks.

Figure 1 shows the correlation plot of the ^{13}C chemical shift (CS) values, calculated at HF level versus the corresponding experimental data of the fourteen species shown in Scheme 1.



Scheme 2. Correct and incorrect structures for antidesmone (**15**,^[9] **16**^[12]), magnolialide (**17**,^[16] **18**–**19**^[13–14]) and benzofurano-eremophil-1-ene (**20**,^[10] **21**^[15]).

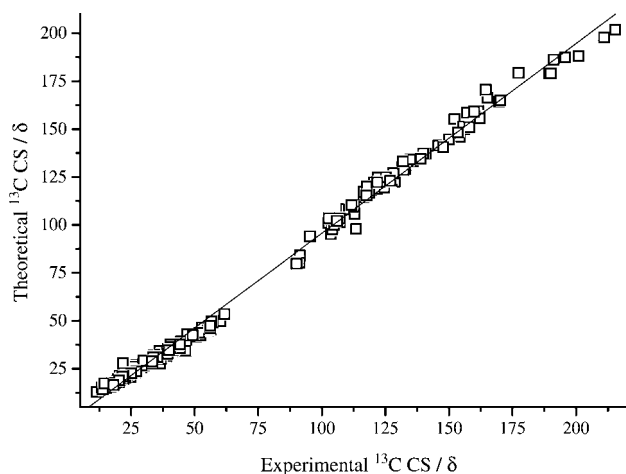


Figure 1. Correlation plot of calculated versus experimental ^{13}C NMR chemical shift (CS), at the HF level, for the species **1**–**14** represented in Scheme 1.

The plot consists of 223 points. The least-squares fit values of intercept, slope and linear correlation coefficient (r) of these points (average) and of the points relative to the single species are reported in Table 1.

At HF level, the r values of the linear fits generally turned out to be greater than or equal to 0.995. In our opinion, this provides a value for comparison with results of analogous calculations that may be employed for ^{13}C NMR structure interpretation.

Nevertheless, a certain variability in the calculated fitting linear parameters has been observed for each of the compounds reported in Table 1, especially in the intercept values.

This, in our opinion, should be attributed to a) electron correlation and b) solvent effects. To verify the weight of these two contributions, in Figure 2 we considered, as an example, the correlation plots of the calculated ^{13}C NMR chemical shifts at both the HF and B3LYP levels, with the experimental data relative to the species 5- α -androstan-12-one (**2**) and coumestane (**8**) (Scheme 1).

The geometry of 5- α -androstan-12-one (**2**) was optimized in the “chair” conformation for the three cyclohexyl groups, and the calculated ^{13}C NMR chemical shifts showed a high correlation with the corresponding experimental data. The observed ^{13}C NMR chemical shift values, except the one relative to the keto function at C-12, fell in the high-field range $\delta = 10$ –60 ppm (see Figure 2).

Table 1. Intercept, slope, correlation coefficient (r) and corresponding HF and B3LYP energy, obtained by linear fitting of calculated versus experimental ^{13}C NMR chemical shift plots for the species in Scheme 1.

Species	Theory	Intercept	Slope	r	Energy [a.u.]
1	HF	–5.650	1.008	0.995(5)	–1099.9125
2	HF	–2.080	0.933	0.998(0)	–811.8504
	B3LYP	3.530	0.934	0.999(8)	–817.3365
3	HF	–2.060	0.936	0.998(2)	–811.8499
4	HF	–1.252	0.996	0.999(5)	–387.9785
5	HF	–2.068	0.985	0.997(1)	–387.9604
6	HF	0.758	0.955	0.999(7)	–462.8238
7	HF	0.556	0.956	0.999(7)	–462.8236
8	HF	4.285	0.950	0.989(2)	–797.3028
	B3LYP	2.443	0.934	0.996(4)	–802.1093
9	HF	–3.278	0.974	0.994(7)	–775.9779
10	HF	–3.568	0.981	0.997(1)	–775.9683
11	HF	–3.594	0.992	0.995(5)	–775.9673
12	HF	–5.551	1.029	0.997(8)	–842.3934
13	HF	3.985	0.747	0.995(8)	–661.2445
14	HF	–5.810	1.011	0.997(4)	–1562.2763
	HF	–3.265	0.990	0.997(6)	–
	average				

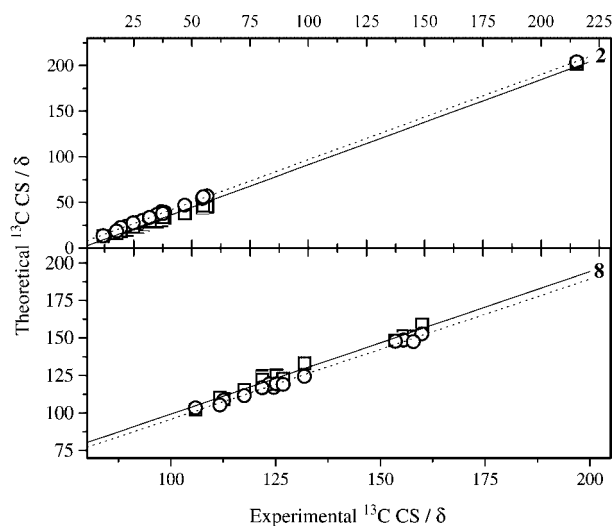


Figure 2. Two examples of correlation plots, data points, and fitting straight lines, of calculated versus experimental ^{13}C NMR chemical shift (CS), at the HF (solid lines, square boxes) and the B3LYP (dotted lines, round boxes) levels, for 5- α -androstan-12-one (**2**) and coumestane (**8**).

The carbon atom C-12 in **2** is more deshielded as a consequence of the binding to the oxygen atom. The values for the intercept, slope and r of the corresponding linear fits for (**2**) and (**8**) are reported in Table 1. The lowest r value observed for coumestane (**8**) at the HF level, 0.989 (see Figure 2 and Table 1), has to be, as reported for similar compounds,^[4,5] attributable to the presence of extensive electron conjugation and lone pairs of electrons on the oxygen atoms. This is related to the low-field region ($\delta = 110$ – 170 ppm) of the experimental ^{13}C NMR chemical shift signals (see Figure 2).

In this case, the requirement of post-HF methods for its treatment seems to be necessary; in fact the linear correlation of the chemical shifts calculated at the B3LYP level turned out to be higher: 0.996 (see Figure 2 and Table 1). On the other hand, chemical shifts of **2** calculated at the B3LYP level did not produce relevant improvements in the r values with respect to the chemical shifts calculated at the HF level (Figure 2 and Table 1). These results indicate that, in the ab initio determination of ^{13}C NMR parameters, 1) the electron correlation energy contribution, as expected, increases with the electron density around the carbon atoms since at the B3LYP level we significantly improve the linear correlation observed at the HF level, and 2) for the particular class of low-polar compounds investigated here, the solvent effects should be negligible.

To verify the reliability of the method, we considered three general cases of misinterpretation of ^{13}C NMR spectra, with incorrect structure assignments. These concerned the alkaloid antidesmone (**15**),^[9] a *Cichorium* sesquiterpene lactone (**12**)^[7] and a sesquiterpene from *Ligularia sagitta* (**20**),^[10] represented in Scheme 2. In the original papers^[7,9,10] it is stressed that the small amount of sample and the structural complexity of natural products can cause the lack of key diagnostic NMR correlations in the two-dimensional spectra necessary for a safe assignment. In these cases, a validation method for structure elucidation of natural compounds could be a powerful supporting tool to avoid incorrect structural inter-

pretations of experimental NMR data. For this purpose, we calculated ^{13}C NMR chemical shift values by the method described here, at both the HF and the B3LYP level, for the right and wrong structures for the compounds listed above (see Scheme 2).^[7,9,10,12–15]

Antidesmone: In a recent paper,^[9] the structure of antidesmone, an alkaloid from *Antidesma membranaceum* and *Antidesma venosum*, was revised to become structure **15** (Scheme 2), rather than the isoquinoline derivative **16**, as assumed previously.^[12] To explore the potential of the validation method proposed, structures **15** and **16**, for which the octyl fragment at C-6 was substituted in our calculation by the shorter propyl group, were optimized at the HF and the B3LYP level and ^{13}C NMR chemical shifts were determined. Figure 3 shows the calculated and corresponding experimental ^{13}C NMR chemical shift^[9] The values of intercept, slope, and r of the least-squares linear fits are reported in Table 2.

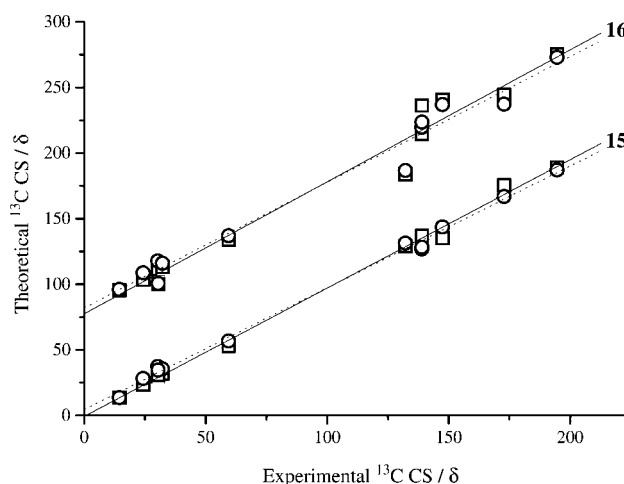


Figure 3. Correlation plots of calculated versus experimental ^{13}C NMR chemical shift (CS), data points, and fitting straight lines, at the HF (solid lines, square boxes) and the B3LYP (dotted lines, round boxes) levels, for the right (**15**) and wrong (**16**) proposed structures of antidesmone. The plot relative to **16** has been displaced by 80 ppm along the ordinate axis, for better visualization.

Table 2. Intercept, slope, correlation coefficient (r) and corresponding HF and B3LYP energy, obtained by linear fitting of calculated versus experimental ^{13}C NMR chemical shift plots for the species in Scheme 2.

Species	Theory	Intercept	Slope	r	Energy [a.u.]
15	HF	-0.812	0.979	0.998(4)	-820.2571
	B3LYP	4.438	0.928	0.998(2)	-825.3624
16	HF	-2.591	1.006	0.985(6)	-820.2679
	B3LYP	1.990	0.957	0.988(3)	-825.3699
17	HF	-2.960	0.979	0.996(3)	-804.2320
	B3LYP	2.843	0.945	0.998(8)	-809.2810
18	HF	-2.922	0.982	0.993(8)	-804.2305
	B3LYP	3.611	0.941	0.996(3)	-809.2789
19	HF	-1.543	0.988	0.992(3)	-804.2343
	B3LYP	4.789	0.946	0.992(1)	-809.2830
20	HF	0.302	0.978	0.999(4)	-652.1924
	B3LYP	3.418	0.933	0.999(5)	-656.4519
21	HF	1.981	0.968	0.999(0)	-652.1857
	B3LYP	5.319	0.920	0.999(4)	-656.4437
	HF	-2.365	0.988	0.997(8)	-
	average				
	B3LYP	3.600	0.931	0.999(2)	-

The r value, relative to structure **15**, is higher than that observed for structure **16**. In particular, the r value of the latter, 0.986, is lower than the average value reported in Table 1. This would indicate that **16** is a less probable structure than **15** for antidesmone. To confirm this hypothesis we employed another parameter useful for discriminating between the trial structures. This was obtained by considering the differences between scaled theoretical and experimental ^{13}C chemical shift values ($\Delta\delta$). The scaled theoretical chemical shift value of any X carbon atom of a given compound, CS_{SX} , was obtained as: $\text{CS}_{\text{SX}} = (\text{CS}_X - \text{Intercept})/\text{Slope}$, *Intercept* and *Slope* being the corresponding least-squares parameters obtained by the linear correlation plots of the same compound. The $\Delta\delta$ values for each carbon atom of structures **15** and **16** of Scheme 2, are shown in Figure 4. Considering the

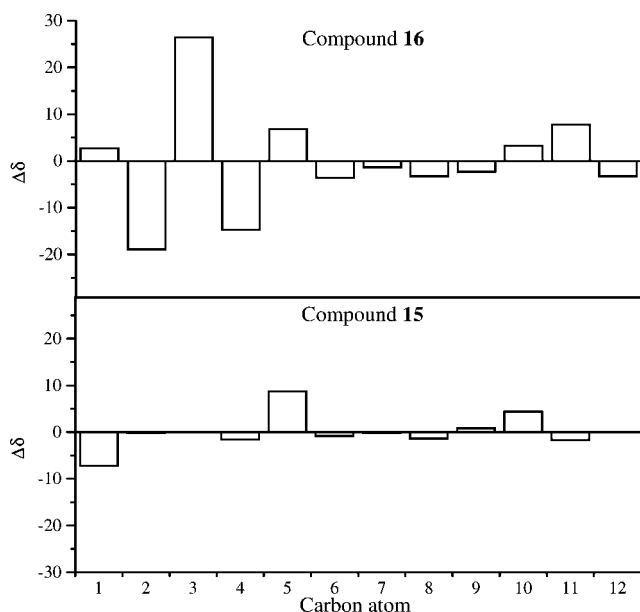


Figure 4. Differences between scaled and experimental ^{13}C NMR chemical shifts for the right (**15**) and wrong (**16**) proposed structures of antidesmone.

$\Delta\delta$ values of structure **16** for the single carbon atoms, it is possible to appreciate considerable deviations for C-2, C-3, and C-4: $\delta = 18.9$, 26.4, and 14.7 ppm respectively (see Figure 4). Thus structure **16** is finally ruled out on the basis of this evidence.

The B3LYP calculations of ^{13}C chemical shifts confirm the trends observed at HF level (see Table 2, rows 15 and 16).

Magnolialide: The *Cichorium* eudesmanolide magnolialide was first isolated from *Magnolia grandiflora* in 1979 and reported as structure **17** (Scheme 2). Its structure elucidation was confirmed by comparison with a synthetic product obtained by cyclization of costunolide-1,10-epoxide.^[16] The same compound was later isolated from *Cichorium intybus*, *Cichorium endivia*^[13] and *Cichorium pumilum*^[14] and assigned wrongly to structures **18** and **19**, respectively. On the basis of the results reported in Figure 5 and in Table 2, for compounds **17**, **18**, and **19**, we observe that compound **19** shows the lowest correlation coefficient among the three. This, and the very large values of $\Delta\delta$ corresponding to the atoms C-5, C-8, C-13,

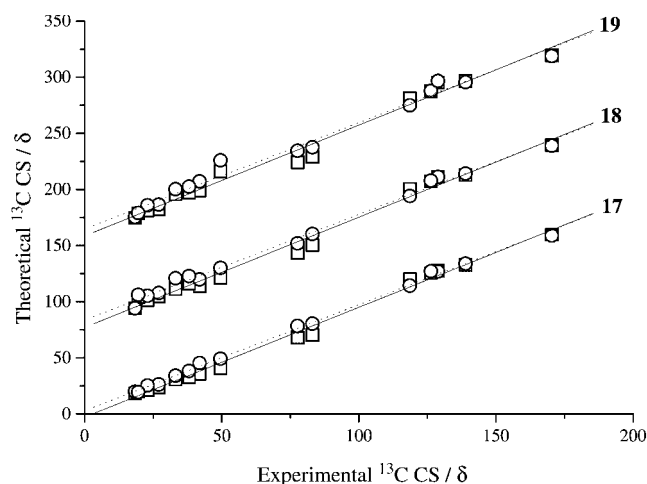


Figure 5. Correlation plots of calculated versus experimental ^{13}C NMR chemical shift, data points, and fitting straight lines, at the HF (solid lines, square boxes) and the B3LYP (dotted lines, round boxes) levels, for the right (**17**) and wrong (**18** and **19**) proposed structures of magnolialide. The plots relative to **18** and **19** have been displaced, respectively, by 80 and 160 ppm along the ordinate axis, for better visualization.

and C-14, allows one to exclude **19** as a possible structure of magnolialide.

The $\Delta\delta$ plots of **17** and **18** are quite similar, as shown in Figure 6. However, the $\Delta\delta$ values are slightly larger for **18**. This, together with the r values obtained from the correlation

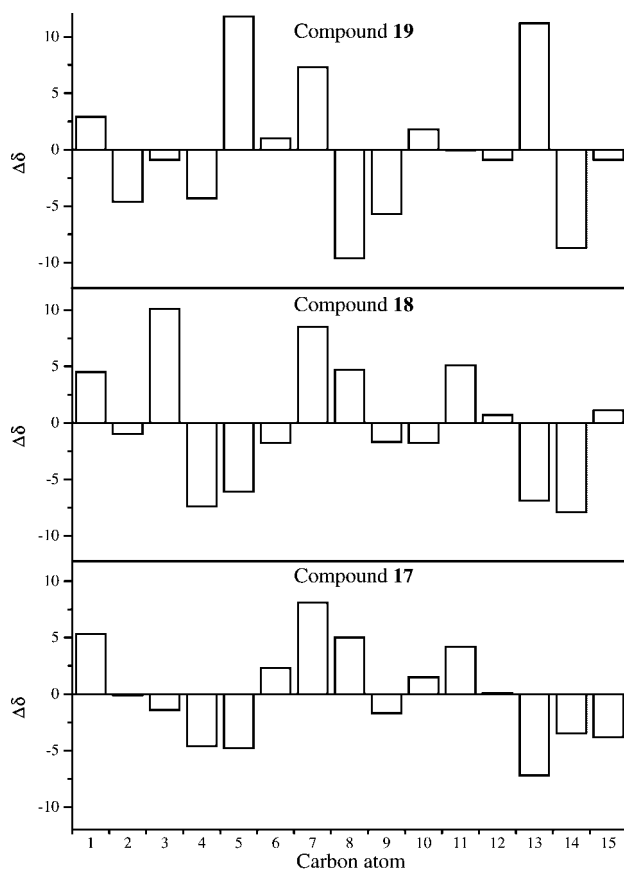


Figure 6. Differences between scaled and experimental ^{13}C NMR chemical shifts for the right (**17**) and wrong (**18** and **19**) proposed structures of antidesmone.

plots of these compounds (Table 2) led to the assignment of structure **17** to magnolialide.

This analysis is supported by the correlation plots obtained from the chemical shift data calculated at B3LYP level (see Figure 5 and Table 2).

Incidentally, it should be noted that, by our computational approach, we have been able to discriminate between and assign the chemical shift values $\delta = 128.87$ and 126.34 ppm to the C-4 and C-5 of magnolialide (**17**), respectively, which had not been unequivocally assigned previously.^[7]

Sesquiterpenes from *Ligularia sagitta*: An intrinsic limitation of the present method occurs when the ^{13}C calculated chemical shift values of correct and incorrect structures are very similar. This is the case for compounds **20** and **21** (Scheme 2), both considered for the interpretation of the ^{13}C NMR spectrum of the sesquiterpene isolated from the rhizomes of *Ligularia sagitta*.^[15] The revised structure **21** differs from the correct **20** in only the position of a double bond; C-2/C-3 in **21** moved to C-1/C-2 in **20**. Indeed, for both structures **20** and **21** the relative r values are higher than 0.999 (Figure 7 and Table 2), the one observed for **20** being slightly

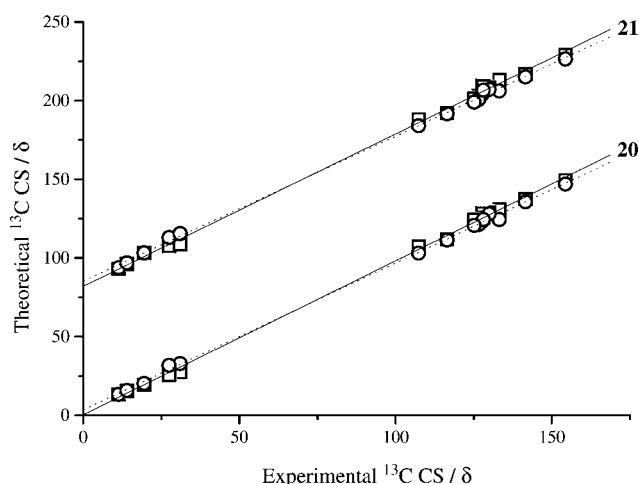


Figure 7. Correlation plots of calculated versus experimental ^{13}C NMR chemical shift (CS), data points, and fitting straight lines, at the HF (solid lines, square boxes) and the B3LYP (dotted lines, round boxes) levels, for structures, right (**20**) and wrong (**21**), of *ligularia*. The plot relative to **21** has been displaced by 80 ppm along the ordinate axis, for better visualization.

larger than that observed for **21** at both the HF and B3LYP levels. Neither value, nor the $\Delta\delta$ analysis, allow in this case an unambiguous assignment. However, the correct assignment of structure **20** was achieved by the joint analysis of two-dimensional NMR experiments and X-ray crystallographic results.^[10]

Further considerations on HF and B3LYP calculations of ^{13}C NMR chemical shifts: Figure 1 shows that the straight lines fitting the points in the range 10–70 ppm of the experimental chemical shift axis would have a lower linear slope and a higher intercept than those fitting the data included in the range $\delta = 90$ –220 ppm. An example is given by podocarpene (**13**), whose ^{13}C chemical shift values range within 10–60 ppm. In this case, the slope and intercept

calculated at the HF level were lower and higher with respect to the average values (Table 1, row 13 and 15, respectively). Moreover, the points in the range 90–220 ppm in the experimental chemical shift axis are quite scattered as observed, for example, in the case of coumestane (**8**), (Figure 2 and Table 1, row 8), whose ^{13}C NMR signals fall in the low-field range 110–170 ppm. This behavior can be attributed to electron correlation effects, which produce two different linear trends in these two regions of the ^{13}C NMR spectrum. Figure 8 shows two overlapped correlation plots obtained by considering the compounds reported in Scheme 2 together with the data relevant to **8** and **2**, see Scheme 1 and Table 1.

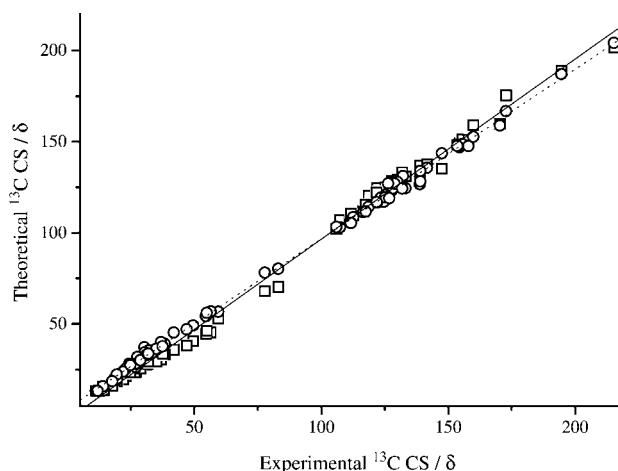


Figure 8. Correlation plots of calculated versus experimental ^{13}C NMR chemical shift (CS), data points, and fitting straight lines, at the HF (solid lines, square boxes) and the B3LYP (dotted lines, round boxes) levels, for the species **2**, **8**, **15**–**21**.

The plots in Figure 8 consist of 76 data points and the trend is similar to that of Figure 1. The least-squares fit parameters, reported in Table 2, show analogous values of intercept, slope, and r value to the ones reported in Table 1. On the other hand, in Figure 8 it is clearly seen that 1) the departure from the average intercept and slope in the high-field region is clearly reduced at the B3LYP level, together with 2) the scattering of data observed in the low-field region. This, in our opinion, would indicate that both of the above effects could be mainly attributed to the neglect of electron correlation at the HF level; the solvent interaction effects less affect the chemical shift calculations.

Interestingly, the calculated chemical shifts were usually lower than the corresponding experimental ones (see Supporting Information). This has to be related to the variation principle followed by HF methods.^[17] In fact, by improving the level of the theoretical method, the ^{13}C NMR chemical shifts usually increase as the total energy of the system decreases, approaching the experimental values.^[3, 4, 6] This led us to assume that differential calculated chemical shift values (see Computational Methods) should be preferable to calculated magnetic shielding values, if the same level of theory for geometry optimization and ^{13}C chemical shift calculation is employed.^[5] In fact, in this way we should partially compen-

sate for systematic errors of the calculated with respect to the experimental data, due to correlation energy contributions.

Conclusion

The HF and B3LYP methods are proposed here as a computational tool to support the structural interpretation of NMR data of low-polar, medium-sized, natural products.

GIAO-calculated chemical shift values of optimized trial structures were used to draw linear correlation plots of calculated versus experimental ^{13}C NMR data. The correlation plot parameters and/or their functional expression allowed confident structural interpretations of NMR spectra.

At the HF level, with the 6-31G(d) basis set, an r value of about 0.995 is generally indicative of a judicious guess. Slope and intercept of the different linear fits show a large range of values, depending on the considered range of NMR ^{13}C chemical shift. Compounds presenting extensive electron conjugation and/or lone pairs of electrons, show ^{13}C NMR signals in the low-field region. In such cases, a slightly lower linear correlation has always been observed, which is, however, improved at the B3LYP level.

Of course, limits occur when the ^{13}C NMR interpretation is based on small-differing trial structures. In this case the use of appositely defined $\Delta\delta$ parameters was suggested.

Computational Methods

Ab initio calculations were performed on the species indicated in Scheme 1 and 2 at the HF and at the B3LYP level, with the 6-31G(d) basis set, using the Gaussian98W package.^[18] The geometry of the species above, together with that of tetramethylsilane (TMS), were fully optimized. The theoretical NMR ^{13}C chemical shift values were obtained by subtracting the GIAO-calculated^[19–21] ^{13}C isotropic magnetic shielding (I.M.S.) of any X carbon atom, to the average GIAO ^{13}C IMS of TMS: $\text{CS}_X = \text{IMS}_{\text{TMS}} - \text{IMS}_X$. Least-square linear fitting parameters of correlation plots between computed and experimental chemical shift values and/or a functional expression of the same parameters (see Results and Discussion) were employed to discriminate among the structural hypotheses.

Acknowledgments

The authors thank Ministero dell'Università e della Ricerca Scientifica e Tecnologica and Università di Salerno, Italy, for financial support.

- [1] J. Casanovas, A. M. Namba, S. Leon, G. L. B. Aquino, G. V. J. da Silva, C. Aleman, *J. Org. Chem.* **2001**, *66*, 3775–3782.
- [2] A. B. Sebag, D. A. Forsyth, M. A. Plante, *J. Org. Chem.* **2001**, *66*, 7967–7973.
- [3] D. B. Chesnut, in *Reviews in Computational Chemistry*, vol. 8 (Eds.: K. B. Lipkowitz, D. B. Boyd), VCH, New York, **1996**, ch. 5, p. 245–297.
- [4] A. C. J. de Dios, *Prog. Nucl. Magn. Reson. Spectrosc.* **1996**, *29*, 229–278.
- [5] D. A. Forsyth, A. B. Sebag, *J. Am. Chem. Soc.* **1997**, *119*, 9483–9494.
- [6] T. Helgaker, M. Jaszunski, K. Ruud, *Chem. Rev.* **1999**, *99*, 293–352.
- [7] W. Kisiel, K. Zielinska, *Phytochemistry* **2001**, *57*, 523–527.
- [8] E. Breitmeier, W. Voelter, *Carbon-13 NMR Spectroscopy*, VCH, New York, **1990**.
- [9] G. Bringmann, J. Schlauer, H. Rischer, M. Wohlfarth, J. Muehlbacher, A. Buske, A. Porzel, J. Schmidt, G. Adam, *Tetrahedron* **2000**, *56*, 3691–3695.
- [10] Z. Liu, H. Chen, Z. Jia, N. K. Dalley, X. Kou, D. Li, N. L. Owen, D. M. Grant, *Phytochemistry* **1995**, *40*, 1191–1192.
- [11] G. Barone, D. Duca, A. Silvestri, L. Gomez-Paloma, R. Riccio, G. Bifulco, *Chem. Eur. J.* **2002**, *8*, 3240–3245.
- [12] A. Buske, S. Busemann, J. Muehlbacher, J. Schmidt, A. Porzel, G. Bringmann, G. Adam, *Tetrahedron* **1999**, *55*, 1079–1086.
- [13] M. Seto, T. Miyase, K. Umehara, A. Ueno, Y. Hirano, N. Otani, *Chem. Pharm. Bull.* **1988**, *36*, 2423–242.
- [14] S. El-Masry, N. M. Ghazy, F. Bohlmann, C. Zdero, *Phytochemistry* **1984**, *23*, 1105–110.
- [15] H. Chen, Z. Yang, L. Jia, *Phytochemistry* **1992**, *31*, 2146–214.
- [16] F. S. El-Ferally, Y. M. Chan, D. A. Benigni, *Phytochemistry* **1979**, *18*, 881–888.
- [17] I. N. Levine, *Quantum Chemistry*, V ed., Prentice Hall, Upper Saddle River, NJ, ch. 8, **2000**.
- [18] M. J. Frisch, G. W. Trucks, H. B. Schlegel, G. E. Scuseria, M. A. Robb, J. R. Cheeseman, V. G. Zakrzewski, J. A. Montgomery, R. E. Stratmann, J. C. Burant, S. Dapprich, J. M. Millam, A. D. Daniels, K. N. Kudin, M. C. Strain, O. Farkas, J. Tomasi, V. Barone, M. Cossi, R. Cammi, B. Mennucci, C. Pomelli, C. Adamo, S. Clifford, J. Ochterski, G. A. Petersson, P. Y. Ayala, Q. Cui, K. Morokuma, D. K. Malick, A. D. Rabuck, K. Raghavachari, J. B. Foresman, J. Cioslowski, J. V. Ortiz, B. B. Stefanov, G. Liu, A. Liashenko, P. Piskorz, I. Komaromi, R. Gomperts, R. L. Martin, D. J. Fox, T. Keith, M. A. Al-Laham, C. Y. Peng, A. Nanayakkara, C. Gonzalez, M. Challacombe, P. M. V. Gill, B. G. Johnson, W. Chen, M. W. Won, J. L. Andres, M. Head-Gordon, E. S. Replogle, J. A. Pople, Gaussian 98, Revision A.8, Gaussian, Inc. Pittsburgh PA, **1998**.
- [19] R. Ditchfield, *Mol. Phys.* **1974**, *27*(4), 789–807.
- [20] C. M. Rohlfing, L. C. Allen, R. Ditchfield, *Chem. Phys.* **1984**, *87*, 9–15.
- [21] K. Wolinski, J. F. Hinton, P. Pulay, *J. Am. Chem. Soc.* **1990**, *112*, 8251–8260.

Received: December 17, 2001

Revised: March 27, 2002 [F3744]